Supplementary Materials for

Reactivation of PTEN tumor suppressor for cancer treatment through inhibition of a MYC-WWP1 inhibitory pathway

Yu-Ru Lee, Ming Chen, Jonathan D. Lee*, Jinfang Zhang*, Shu-Yu Lin*, Tian-Min Fu, Hao Chen, Tomoki Ishikawa, Shang-Yin Chiang, Jesse Katon, Yang Zhang, Yulia V. Shulga, Assaf C. Bester, Jacqueline Fung, Emanuele Monteleone, Lixin Wan, Chen Shen, Chih-Hung Hsu, Antonella Papa, John G. Clohessy, Julie Teruya-Feldstein, Suresh Jain, Hao Wu, Lydia Matesic, Ruey-Hwa Chen, Wenyi Wei, Pier Paolo Pandolfi†

*These authors contributed equally to this work.
†Corresponding author. Email: ppandolf@bidmc.harvard.edu

Published 17 May 2019, *Science* **364**, eaau0159 (2019)
DOI: 10.1126/science.aau0159

This PDF file includes:

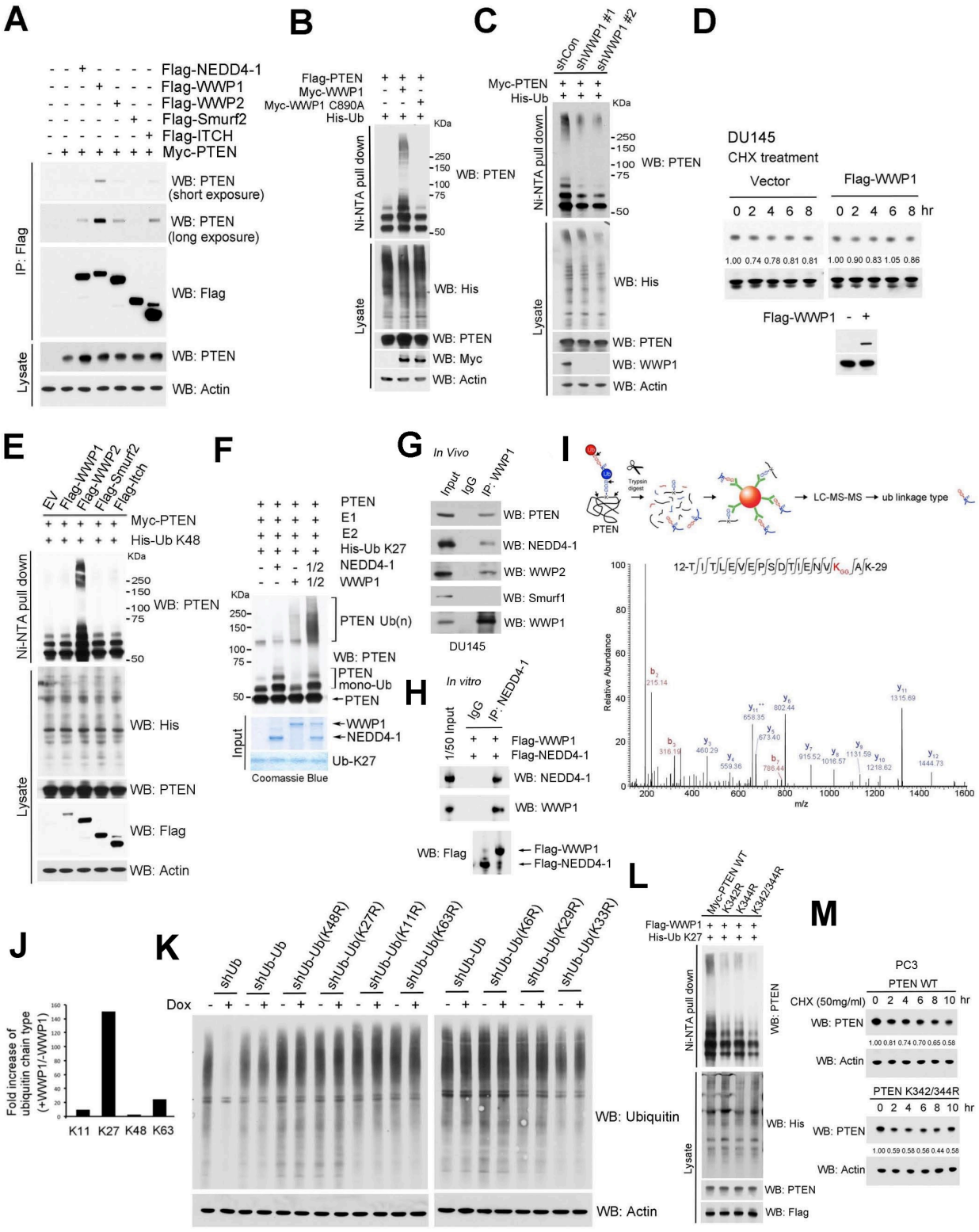
A
Flag-NEDD4-1
Flag-WWP1
Flag-WWP2
Flag-Smurf2
Flag-ITCH
Myc-PTEN
IP: Flag
WB: PTEN (short exposure)
WB: PTEN (long exposure)
WB: Flag
Lysate
WB: PTEN
WB: Actin
B
Flag-PTEN
Myc-WWP1
Myc-WWP1 C890A
His-Ub
KDa
Ni-NTA pull down
WB: PTEN
Lysate
WB: His
WB: PTEN
WB: Myc
WB: Actin
C
shCon
shWWP1 #1
shWWP1 #2
Myc-PTEN
His-Ub
KDa
Ni-NTA pull down
WB: PTEN
Lysate
WB: His
WB: PTEN
WB: WWP1
WB: Actin
D
DU145
CHX treatment
Vector
Flag-WWP1
0 2 4 6 8
0 2 4 6 8 hr
1.00 0.74 0.78 0.81 0.81
1.00 0.90 0.83 1.05 0.86
Flag-WWP1
E
EV
Flag-WWP1
Flag-WWP2
Flag-Smurf2
Flag-Itch
Myc-PTEN
His-Ub K48
KDa
Ni-NTA pull down
WB: PTEN
Lysate
WB: His
WB: PTEN
WB: Flag
WB: Actin
F
PTEN
E1
E2
His-Ub K27
NEDD4-1
WWP1
1/2
1/2
KDa
PTEN Ub(n)
WB: PTEN
PTEN mono-Ub
PTEN
Input
WWP1
NEDD4-1
Ub-K27
Coomassie Blue
G
In Vivo
Input
IgG
IP: WWP1
WB: PTEN
WB: NEDD4-1
WB: WWP2
WB: Smurf1
WB: WWP1
DU145
H
In vitro
1/50 Input
IgG
IP: NEDD4-1
Flag-WWP1
Flag-NEDD4-1
WB: NEDD4-1
WB: WWP1
WB: Flag
Flag-WWP1
Flag-NEDD4-1
I
PTEN
Trypsin digest
LC-MS-MS
ub linkage type
12-T/I/T/L/E/V/E/P/S/D/T/I/E/N/V/K(gg)/A/K-29
Relative Abundance
m/z
J
Fold increase of ubiquitin chain type (+WWP1/-WWP1)
K11
K27
K48
K63
K
shUb
shUb-Ub
shUb-Ub(K48R)
shUb-Ub(K27R)
shUb-Ub(K11R)
shUb-Ub(K63R)
shUb-Ub
shUb-Ub(K6R)
shUb-Ub(K29R)
shUb-Ub(K33R)
Dox
WB: Ubiquitin
WB: Actin
L
Myc-PTEN WT
K342R
K344R
K342/344R
Flag-WWP1
His-Ub K27
Ni-NTA pull down
WB: PTEN
Lysate
WB: His
WB: PTEN
WB: Flag
M
PC3
PTEN WT
CHX (50mg/ml)
0 2 4 6 8 10 hr
WB: PTEN
1.00 0.81 0.74 0.70 0.65 0.58
WB: Actin
PTEN K342/344R
0 2 4 6 8 10 hr
WB: PTEN
1.00 0.59 0.58 0.56 0.44 0.58
WB: Actin

Fig. S1.

(**A**) Co-immunoprecipitation analysis of the interaction between Myc-PTEN and individual Flag-tagged NEDD4 family ubiquitin E3 ligase. Immunoprecipitation (IP) of Flag-NEDD4 family ligases with Flag antibody, and then probed with PTEN antibodies to detect PTEN/individual NEDD4 family ligase interactions.

(**B**) Effects of WWP1 catalytic activity on PTEN poly-ubiquitination. 293T cells were transfected with indicated constructs, and PTEN ubiquitination was analyzed. The ubiquitinated proteins were pulled down under denaturing conditions by Ni-NTA agarose, and analyzed by western blot.

(**C**) Analysis of PTEN K27-linked poly-ubiquitination in DU145 cells stably expressing two independent WWP1 shRNAs. DU145 lysates were transfected with PTEN along with His-ubiquitin (His-Ub); lysates were collected for Ni-NTA pull down, followed by western blot analysis.

(**D**) DU145 cells transfected with indicated constructs were treated with 100 μg/ml cyclohexmide for various time points and endogenous PTEN was analyzed by western blot and ImageJ software.

(**E**) Analysis of PTEN K48-linked poly-ubiquitination in PC3 cells expressing indicated NEDD4 family ubiquitin E3 ligases as in Fig. 1F. PC3 cells were transfected with indicated constructs, treated with 1μM MG132 16 h, and PTEN ubiquitination was analyzed as in Fig. 1F.

(**F**) *In vitro* ubiquitination of PTEN by either NEDD4-1 or WWP1 E3 ligase. Flag-PTEN purified from 293 cells were subjected to *in vitro* ubiquitination reaction in the presence of E1, E2, E3, and His-K27-only ubiquitin, and then examined by western blot with anti-PTEN antibody. The input control of NEDD4-1, WWP1, and ubiquitin before enzymatic reaction was determined by coomassie blue staining, and is shown in the bottom of the figure.

(**G**) WWP1 interacts with PTEN endogenously. DU145 cells were immunoprecipitated with anti-WWP1 antibody and then analyzed by western blot with indicated antibodies.

(**H**) WWP1 binds NEDD4-1 *in vitro*. Recombinant Flag-WWP1 were incubated with immunopurified recombinant NEDD4-1, and then analyzed by western blot.

(**I**) The flow chart of Tandem mass analysis (upper). Tandem mass spectrum of a peptide derived from ubiquitinated PTEN showing ubiquitin conjugation at the K27 residue of ubiquitin (bottom).

(**J**) Ratio of indicated ubiquitin linkages detected by MS analysis of ubiquitinated PTEN purified from WWP1 overexpression cells to that from control (without WWP1 overexpression) cells. The abundance of each ubiquitin linkage was calculated as described in Methods.

(**K**) Analysis of ubiquitin levels in various ubiquitin replacement cells treated with/without 1μg/ml doxycycline.

(**L**) Effects of the indicated KR mutants on WWP1-mediated PTEN poly-ubiquitination. PC3 cells were transfected with indicated constructs, and PTEN ubiquitination was analyzed as in Fig. 1D.

(**M**) PC3 cells transfected with indicated constructs were treated with 100 μg/ml cyclohexmide for various time points and exogenous PTEN was analyzed by western blot and ImageJ software.

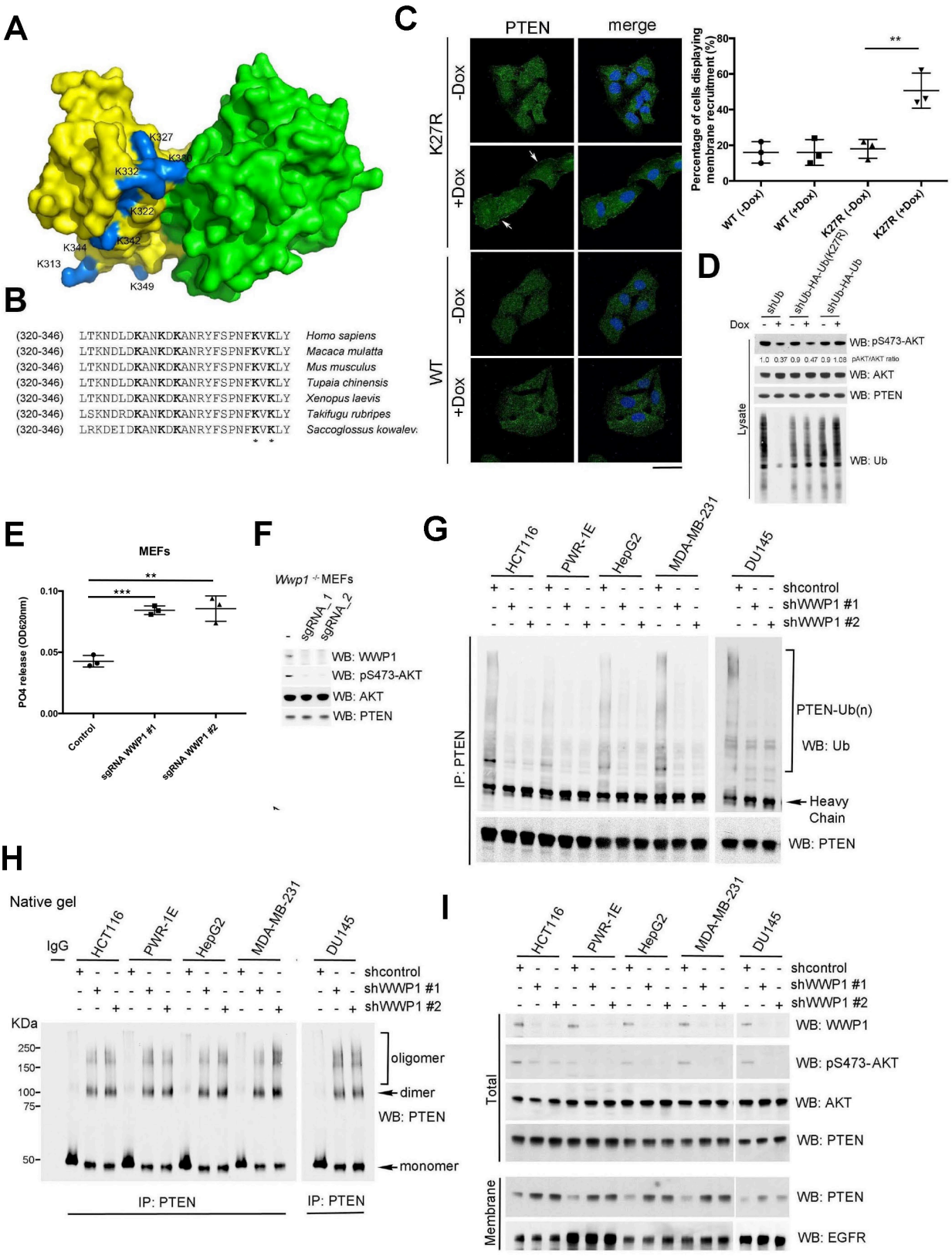
A
K327
K332
K322
K342
K344
K313
K349
B
(320-346) LTKNDLDKANKDKANRYFSPNFKVKLY Homo sapiens
(320-346) LTKNDLDKANKDKANRYFSPNFKVKLY Macaca mulatta
(320-346) LTKNDLDKANKDKANRYFSPNFKVKLY Mus musculus
(320-346) LTKNDLDKANKDKANRYFSPNFKVKLY Tupaia chinensis
(320-346) LTKNDLDKANKDKANRYFSPNFKVKLY Xenopus laevis
(320-346) LSKNDRDKANKDKANRYFSPNFKVKLY Takifugu rubripes
(320-346) LRKDEIDKANKDKANRYFSPNFKVKLY Saccoglossus kowalev
C
PTEN
merge
K27R
WT
-Dox
+Dox
Percentage of cells displaying membrane recruitment (%)
WT (-Dox)
WT (+Dox)
K27R (-Dox)
K27R (+Dox)
D
shUb
shUb-HA-Ub(K27R)
shUb-HA-Ub
Dox
WB: pS473-AKT
pAKT/AKT ratio
WB: AKT
WB: PTEN
Lysate
WB: Ub
E
MEFs
PO4 release (OD620nm)
Control
sgRNA WWP1 #1
sgRNA WWP1 #2
F
Wwp1 -/- MEFs
sgRNA_1
sgRNA_2
WB: WWP1
WB: pS473-AKT
WB: AKT
WB: PTEN
G
HCT116
PWR-1E
HepG2
MDA-MB-231
DU145
shcontrol
shWWP1 #1
shWWP1 #2
IP: PTEN
PTEN-Ub(n)
WB: Ub
Heavy Chain
WB: PTEN
H
Native gel
IgG
KDa
250
150
100
75
50
oligomer
dimer
monomer
WB: PTEN
IP: PTEN
I
Total
Membrane
WB: WWP1
WB: pS473-AKT
WB: AKT
WB: PTEN
WB: EGFR

Fig. S2.

(**A**) 3D structure simulation of PTEN. The N-terminal of PTEN was shown in green, and the C-terminal of PTEN was shown in yellow. The corresponding lysine residues were shown in blue.

(**B**) Conservation of the K342 and K344 patch between different species.

(**C**) Analysis of PTEN subcellular localization in wild type (WT) or K27R ubiquitin replacement cells treated with or without 1 μg/ml doxycycline for 2 Days. Representative confocal images are shown. Arrow indicates the PTEN plasma membrane localization. Bar, 20 μm (left panel). The percentage of cells displaying PTEN plasma membrane localization was quantified (right panel). Data are mean ± SD; triple experiments, fifty cells per group per experiment (***P<0.0005, **P<0.005, triplicate experiments, Student's t-tests).

(**D**) Analysis of AKT activation and ubiquitin expression levels in various ubiquitin replacement cell lines treated with 1 μg/ml doxycycline for 2 Days. The relative amounts of phospho-AKT, normalized to their total levels, are indicated.

(**E**) Effects of indicated WWP1 on PTEN lipid phosphatase activities in MEFs cells with indicated constructs. Data are shown as mean ± SD (***P<0.0005, **P<0.005, triplicate experiments, Student's t-tests).

(**F**) Analysis of AKT activation in *Wwp1*$^{+/+}$ and *Wwp1*$^{-/-}$ MEFs.

(**G**) Analysis of endogenous PTEN ubiquitination in multiple cancer cell lines with stable knockdown of WWP1.

(**H**) To evaluate PTEN dimerization in multiple cancer cells with stable knockdown of WWP1 by Native Gel. Total lysates from cells were immunoprecipitated with a rabbit anti-PTEN antibody, and then the immunocomplexes were natively eluted from the beads. The eluted samples were immediately run on Native Gel.

(**I**) Total and Membrane fractions isolated from multiple cancer cells with stable knockdown of WWP1. EGFR served as a membrane marked, and Actin as the internal control.

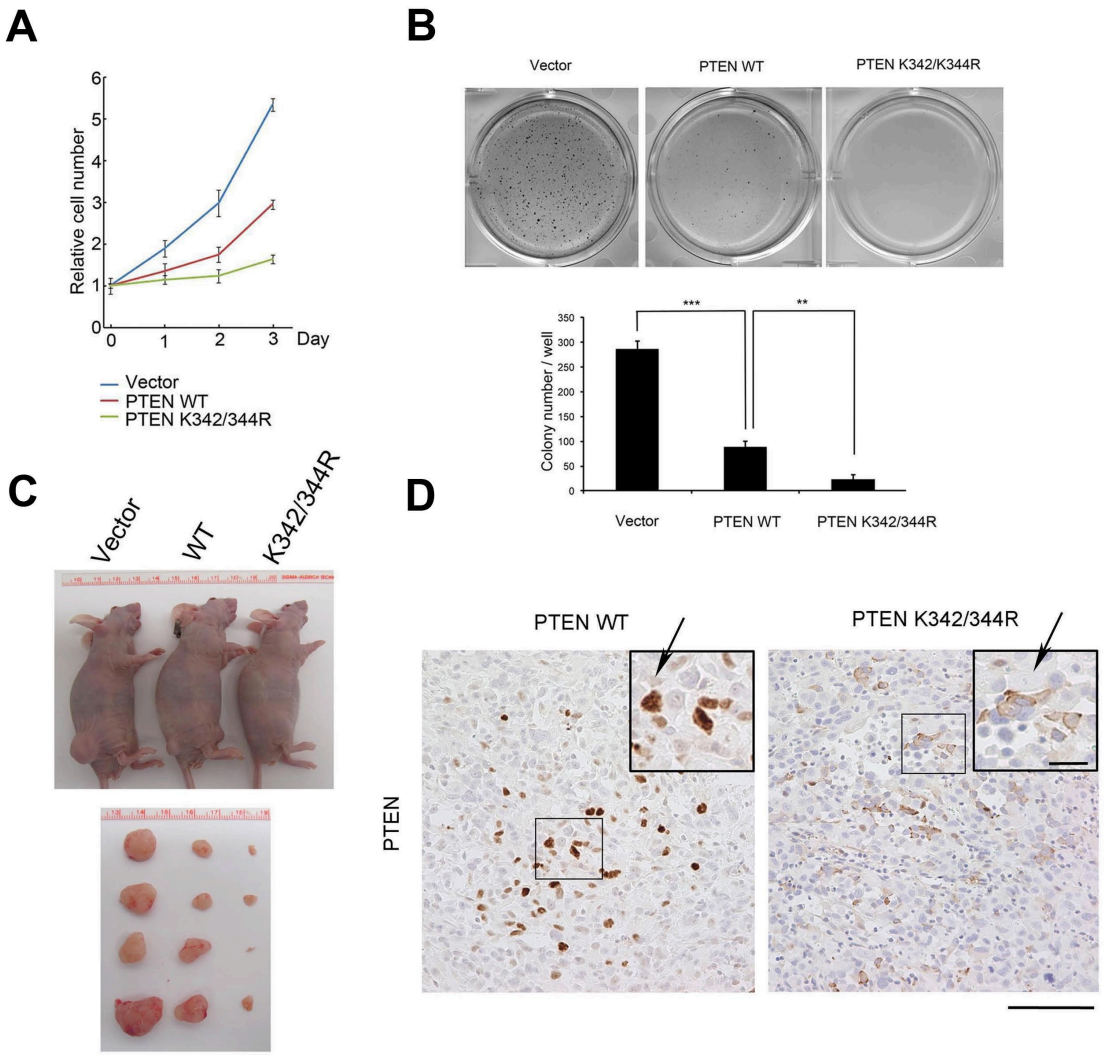

Fig. S3.

(**A**) Effects of PTEN K342/K344R mutant on proliferation of PC3 cells. *In vitro* proliferation rate of PC3 cells as in Fig. 2K.

(**B**) PC3 cells as in Fig. 2K were assayed for their colony forming ability in soft agar. The colony number are quantified and presented as mean ± SD (***P<0.0005, **P<0.005, triplicate experiments, Student's t-tests).

(**C**) Tumor growth of the PC3 cells expressing indicated constructs in a xenograft model.

(**D**) Tumors derived from each cell lines were analyzed by PTEN staining. The boxed areas are enlarged two fold to show on the right. Bar, 50 μm.

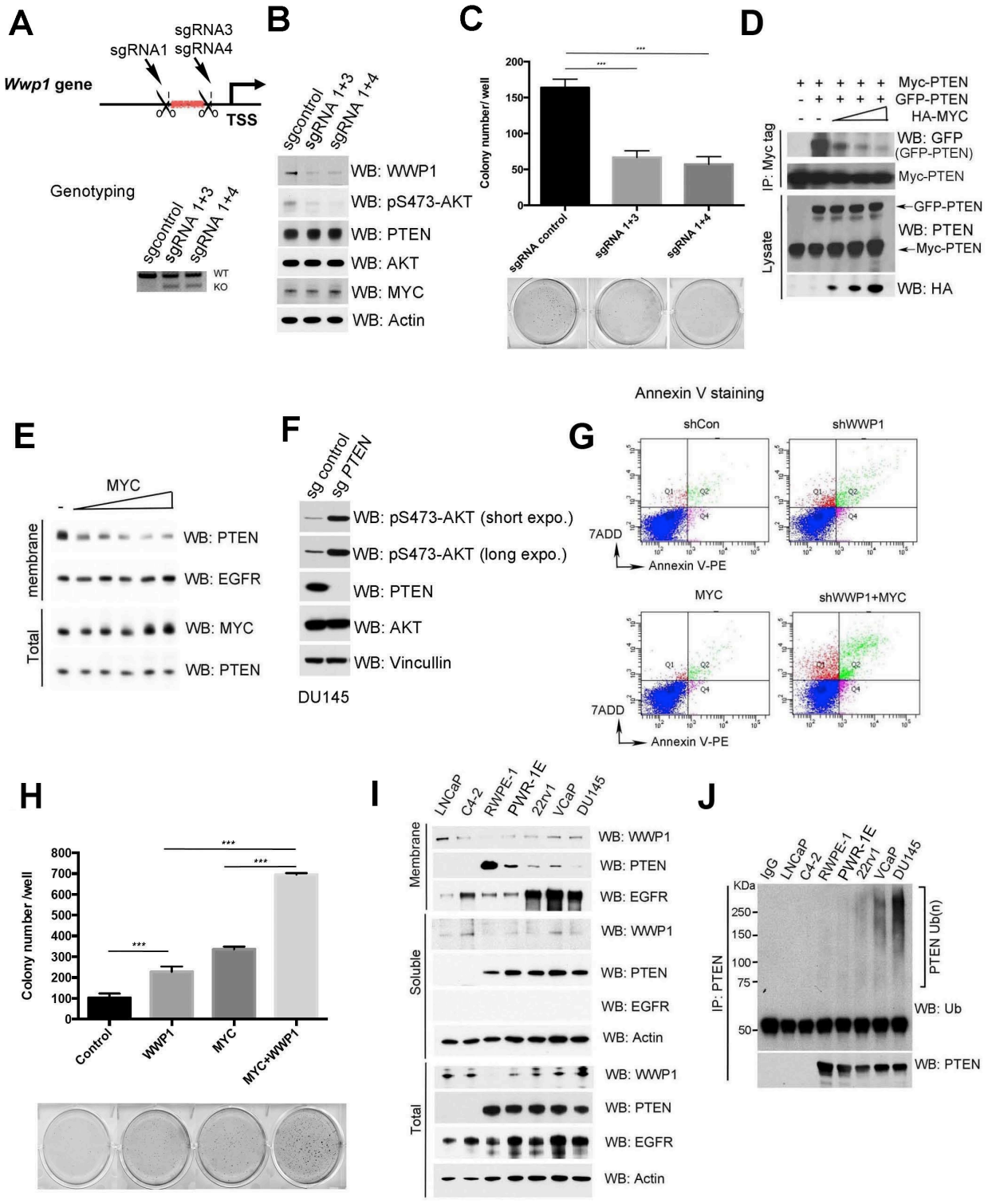
A
sgRNA3
sgRNA1
sgRNA4
Wwp1 gene
TSS
Genotyping
sgcontrol
sgRNA 1+3
sgRNA 1+4
WT
KO
B
sgcontrol
sgRNA 1+3
sgRNA 1+4
WB: WWP1
WB: pS473-AKT
WB: PTEN
WB: AKT
WB: MYC
WB: Actin
C
Colony number/ well
sgRNA control
sgRNA 1+3
sgRNA 1+4
D
Myc-PTEN
GFP-PTEN
HA-MYC
IP: Myc tag
WB: GFP
(GFP-PTEN)
Myc-PTEN
Lysate
GFP-PTEN
WB: PTEN
Myc-PTEN
WB: HA
E
MYC
membrane
WB: PTEN
WB: EGFR
Total
WB: MYC
WB: PTEN
F
sg control
sg PTEN
WB: pS473-AKT (short expo.)
WB: pS473-AKT (long expo.)
WB: PTEN
WB: AKT
WB: Vincullin
DU145
G
Annexin V staining
shCon
shWWP1
7ADD
Annexin V-PE
MYC
shWWP1+MYC
H
Colony number /well
Control
WWP1
MYC
MYC+WWP1
I
LNCaP
C4-2
RWPE-1
PWR-1E
22rv1
VCaP
DU145
Membrane
WB: WWP1
WB: PTEN
WB: EGFR
Soluble
WB: WWP1
WB: PTEN
WB: EGFR
WB: Actin
Total
WB: WWP1
WB: PTEN
WB: EGFR
WB: Actin
J
IgG
LNCaP
C4-2
RWPE-1
PWR-1E
22rv1
VCaP
DU145
KDa
IP: PTEN
PTEN Ub(n)
WB: Ub
WB: PTEN

Fig. S4.

(**A**) Schematic description (upper) and genotyping (bottom) of the CRISPR strategy to remove the MYC responsive element within *WWP1* promoter.

(**B**) Analysis of WWP1 and AKT activation in DU145 cells infected with indicated viruses. Total lysates were resolved by SDS-PAGE and then probed with indicated antibodies.

(**C**) Effects of MYC/WWP1 axis on colony forming ability in soft agar. The colony numbers were quantified and presented as mean ± SD (***P<0.0005, **P<0.005. triplicate experiments, Student's t-tests).

(**D**) Co-immunoprecipitation analysis of the interaction between Myc-PTEN and GFP-PTEN in DU145 cells transfected with the indicated plasmids.

(**E**) Membrane localization of endogenous PTEN in DU145 cells expressing different amount of MYC. Membrane and soluble fractions isolated from cells were analyzed by western blot. EGFR served as a membrane marker.

(**F**) Western blot analysis of DU145 cells with/without *PTEN* knockout by CRISPR.

(**G**) Analysis of apoptosis of DU145 cells stably expressing indicated constructs by staining with Annexin-V-PE and 7ADD, and then followed by FACS analysis.

(**H**) Analysis the coordinative effects of MYC and WWP1 on colony forming ability in soft agar. The colony numbers were quantified and presented as mean ± SD (***P<0.0005, **P<0.005. triplicate experiments, Student's t-tests).

(**I**) Total, membrane, and soluble fractions isolated from different PCa cell lines were analyzed by western blot. EGFR served as a membrane marker, and Actin as the internal control.

(**J**) Analysis of endogenous PTEN ubiquitination in different PCa cell lines.

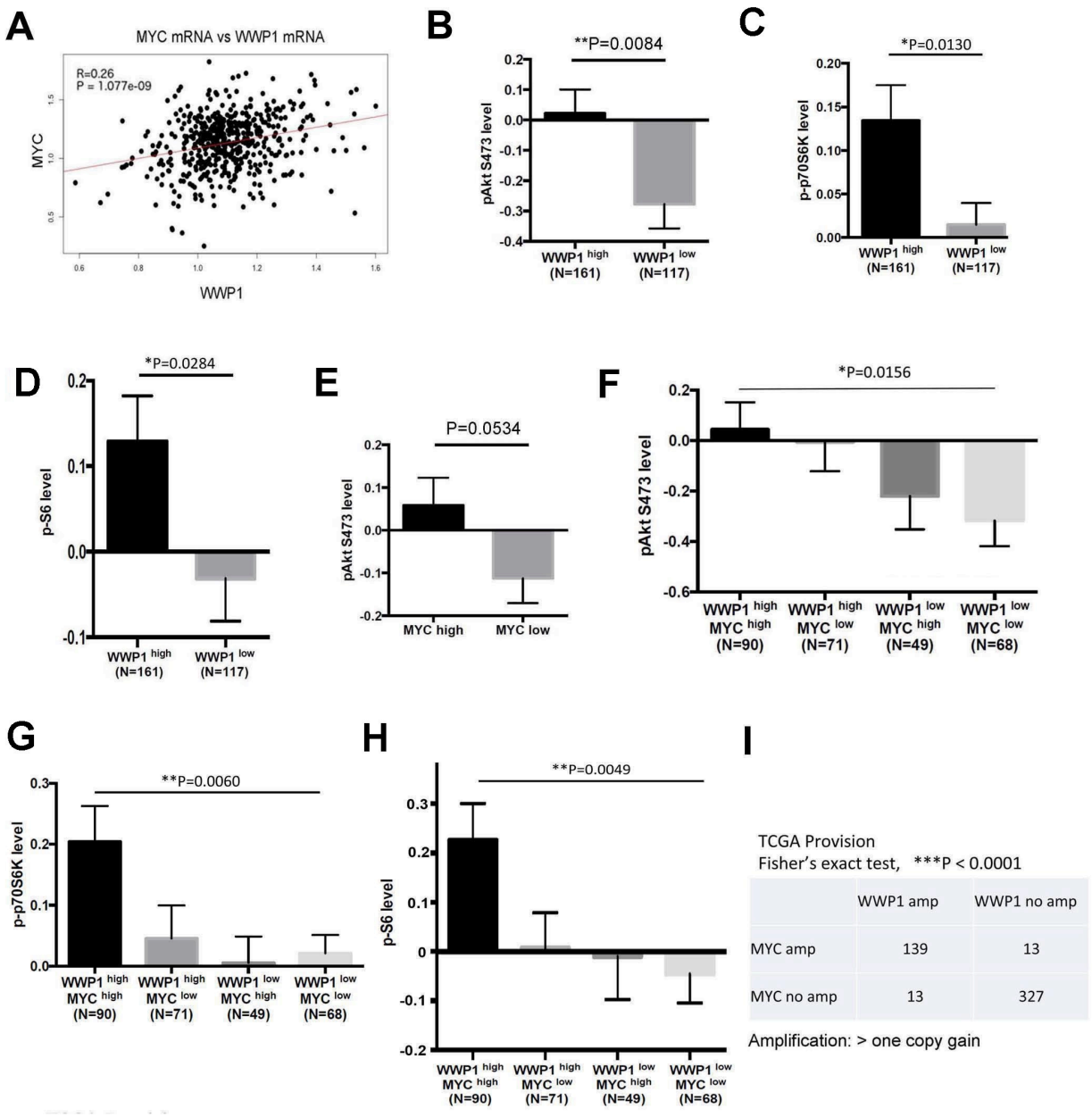
A
MYC mRNA vs WWP1 mRNA
R=0.26
P = 1.077e-09
MYC
WWP1
B
**P=0.0084
pAkt S473 level
WWP1 high (N=161)
WWP1 low (N=117)
C
*P=0.0130
p-p70S6K level
WWP1 high (N=161)
WWP1 low (N=117)
D
*P=0.0284
p-S6 level
WWP1 high (N=161)
WWP1 low (N=117)
E
P=0.0534
pAkt S473 level
MYC high
MYC low
F
*P=0.0156
pAkt S473 level
WWP1 high MYC high (N=90)
WWP1 high MYC low (N=71)
WWP1 low MYC high (N=49)
WWP1 low MYC low (N=68)
G
**P=0.0060
p-p70S6K level
WWP1 high MYC high (N=90)
WWP1 high MYC low (N=71)
WWP1 low MYC high (N=49)
WWP1 low MYC low (N=68)
H
**P=0.0049
p-S6 level
WWP1 high MYC high (N=90)
WWP1 high MYC low (N=71)
WWP1 low MYC high (N=49)
WWP1 low MYC low (N=68)
I
TCGA Provision
Fisher's exact test, ***P < 0.0001
WWP1 amp
WWP1 no amp
MYC amp
139
13
MYC no amp
13
327
Amplification: > one copy gain
J
Robinson., et al Cell 2015
MYC
WWP1
PTEN
Genetic Alteration
K
WWP1 high vs. low
KEGG PI3K/Akt
p-value = 0.03803681
NES = 1.197079
MYC high vs. low
KEGG PI3K/Akt
p-value = 0.01298701
NES = 1.225394
enrichment score
rank

Fig. S5.

(**A**) Expression analysis of between MYC and WWP1 in TCGA data set of human prostate adenocarcinoma. MYC mRNA is positively correlated with WWP1 mRNA.

(**B**) Expression analysis between WWP1 and phospho-AKT (S473) in TCGA RPPA (Reverse Phase Protein Array) of human prostate adenocarcinoma. Data are represented as mean of Z-score ± SEM. (Remove PTEN mRNA low group, Z-score <-2.0). WWP1 is positively correlated with pAKT.

(**C**) Expression analysis between WWP1 and phospho-S6K in TCGA RPPA (Reverse Phase Protein Array) of human prostate adenocarcinoma. Data are represented as mean of Z-score ± SEM. (Remove PTEN mRNA low group, Z-score <-2.0). WWP1 is positively correlated with pS6K.

(**D**) Expression analysis between WWP1 and phospho-S6 in TCGA RPPA (Reverse Phase Protein Array) of human prostate adenocarcinoma. Data are represented as mean of Z-score ± SEM. (Remove PTEN mRNA low group, Z-score <-2.0). WWP1 is positively correlated with pS6.

(**E**) Expression analysis between MYC and phospho-AKT (S473) in TCGA RPPA of human prostate adenocarcinoma. Data are represented as mean of Z-score ± SEM. (Remove PTEN mRNA low group, Z-score <-2.0).

(**F-H**) Protein expression level of pAKT, pS6K, and pS6 in the TCGA RPPA of human prostate adenocarcinoma. Data are represented as mean of Z-score ± SEM. (Remove PTEN mRNA low group, Z-score<-2.0, and the groups are classified by the mRNA expression level of WWP1 and MYC).

(**I**) WWP1 is co-amplified with MYC in human prostate cancer. Co-amplification analysis between MYC and WWP1 in TCGA dataset of human prostate adenocarcinoma.

(**J**) MYC/WWP1 amplification exhibits a mutually exclusive pattern with PTEN deletion/mutation in Robinson dataset (Robinson., et al, Cell, 2015).

(**K**) GSEA analyses of MYC or WWP1 levels with KEGG PI3K-AKT transcriptional outputs in TCGA data set of human prostate adenocarcinoma (Remove PTEN mRNA low group, Z-score <-2.0).

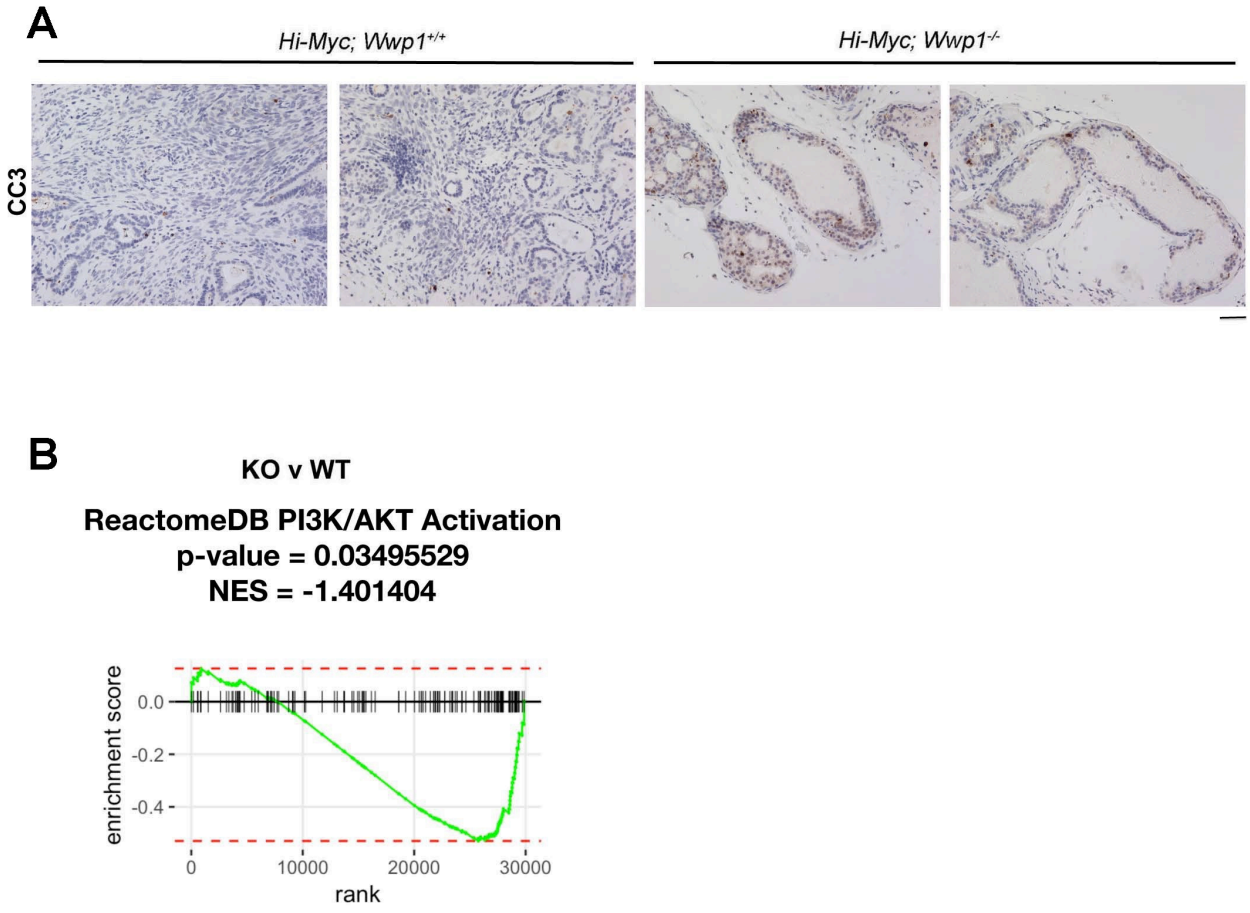

Fig. S6.

(**A**) IHC staining of DLPs from *Hi-Myc; Wwp1*$^{+/+}$ or *Hi-Myc; Wwp1*$^{-/-}$ mice with indicated antibodies. The mice at 5 months of age were analyzed. Scale bar, 50 μm.

(**B**) Gene set enrichment analysis (GSEA) of RNA-Seq data from the DLP prostates of *Wwp1* knockout versus *Wwp1* wild type mice using the PI3K-AKT signaling pathway gene set annotated in the ReactomeDB. Mice from all four groups contain the same Hi-Myc genetic background unless otherwise noted.

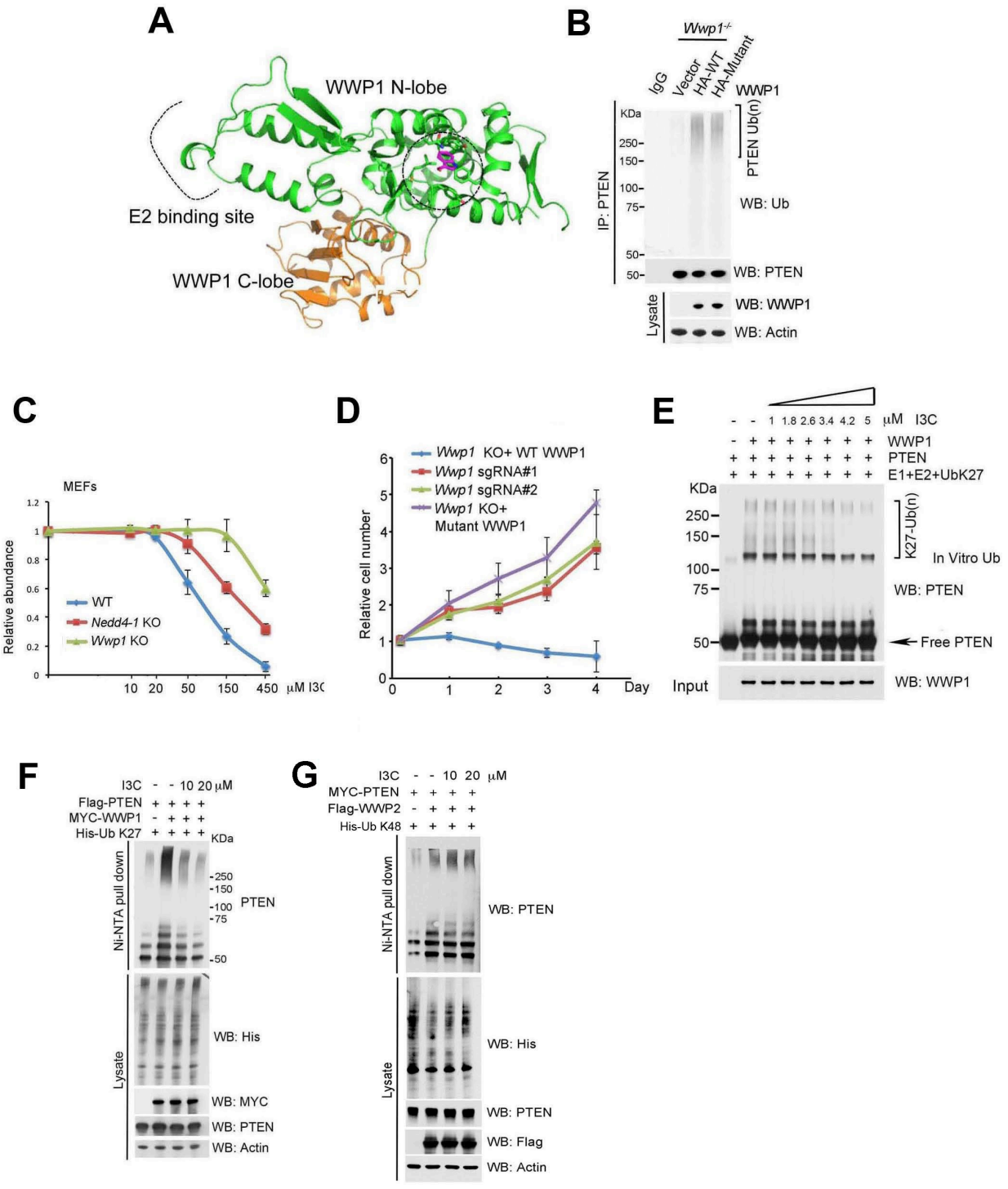
A
WWP1 N-lobe
E2 binding site
WWP1 C-lobe
B
Wwp1-/-
IgG
Vector
HA-WT
HA-Mutant
WWP1
KDa
250
150
100
75
50
50
PTEN Ub(n)
IP: PTEN
WB: Ub
WB: PTEN
Lysate
WB: WWP1
WB: Actin
C
MEFs
Relative abundance
1.2
1
0.8
0.6
0.4
0.2
0
WT
Nedd4-1 KO
Wwp1 KO
10 20 50 150 450 μM I3C
D
Wwp1 KO+ WT WWP1
Wwp1 sgRNA#1
Wwp1 sgRNA#2
Wwp1 KO+
Mutant WWP1
Relative cell number
6
5
4
3
2
1
0
0 1 2 3 4 Day
E
- - 1 1.8 2.6 3.4 4.2 5 μM I3C
- + + + + + + + WWP1
+ + + + + + + + PTEN
+ + + + + + + + E1+E2+UbK27
KDa
250
150
100
75
50
K27-Ub(n)
In Vitro Ub
WB: PTEN
Free PTEN
Input
WB: WWP1
F
I3C - - 10 20 μM
Flag-PTEN + + + +
MYC-WWP1 - + + +
His-Ub K27 + + + +
KDa
Ni-NTA pull down
250
150
100
75
50
PTEN
Lysate
WB: His
WB: MYC
WB: PTEN
WB: Actin
G
I3C - - 10 20 μM
MYC-PTEN + + + +
Flag-WWP2 - + + +
His-Ub K48 + + + +
Ni-NTA pull down
WB: PTEN
Lysate
WB: His
WB: PTEN
WB: Flag
WB: Actin

Fig. S7.

(**A**) Ribbon diagram of WWP1 HECT domain in complex with I3C. The N-lobe of WWP1 HECT domain was shown in green, and the C-lobe of WWP1 HECT domain was shown in orange.

(**B**) Effects of WWP1 WT or WWP1 I3C binding mutant (F577/Y565A) on endogenous PTEN ubiquitination in MEFs. Analysis of endogenous PTEN ubiquitination levels in *Wwp1*$^{-/-}$ MEFs stably expressing indicated constructs.

(**C**) Growth inhibition of *WT*, *Wwp1*$^{-/-}$, and *Nedd4-1*$^{-/-}$ MEFs treated with various days of I3C for 2 days. Representative pictures of the cells at Day 2 are shown below (triplicate experiments).

(**D**) Growth curves of *Wwp1*$^{-/-}$ and *Wwp1*$^{-/-}$ cells stably expressing either WT WWP1 or WWP1 F577/Y656A mutant treated with 60 μM I3C every other day.

(**E**) Inhibition of WWP1-mediated PTEN K27-linked poly-ubiquitination by I3C *in vitro*. Flag-PTEN purified from 293 cells was subject to in vitro ubiquitination reaction in the presence of E1, E2, E3, K27-only ubiquitin, and various concentrations of I3C and then examined by western blot with anti-PTEN antibody. The input control of WWP1 was determined by western blotting, and is shown in the bottom.

(**F**) Effects of I3C on WWP1-mediated PTEN K27-linked poly-ubiquitination. DU145 cells expressing indicated plasmids were treated with different doses of I3C every other day for 4 Days. The ubiquitinated PTEN was pulled down under denaturing conditions by Ni-NTA agarose and analyzed by the western blot.

(**G**) Effects of I3C on WWP2-mediated PTEN K48-linked poly-ubiquitination. DU145 cells expressing indicated plasmids were treated with different doses of I3C every other day for 4 Days. The ubiquitinated PTEN was pulled down under denaturing conditions by Ni-NTA agarose and analyzed by the western blot.

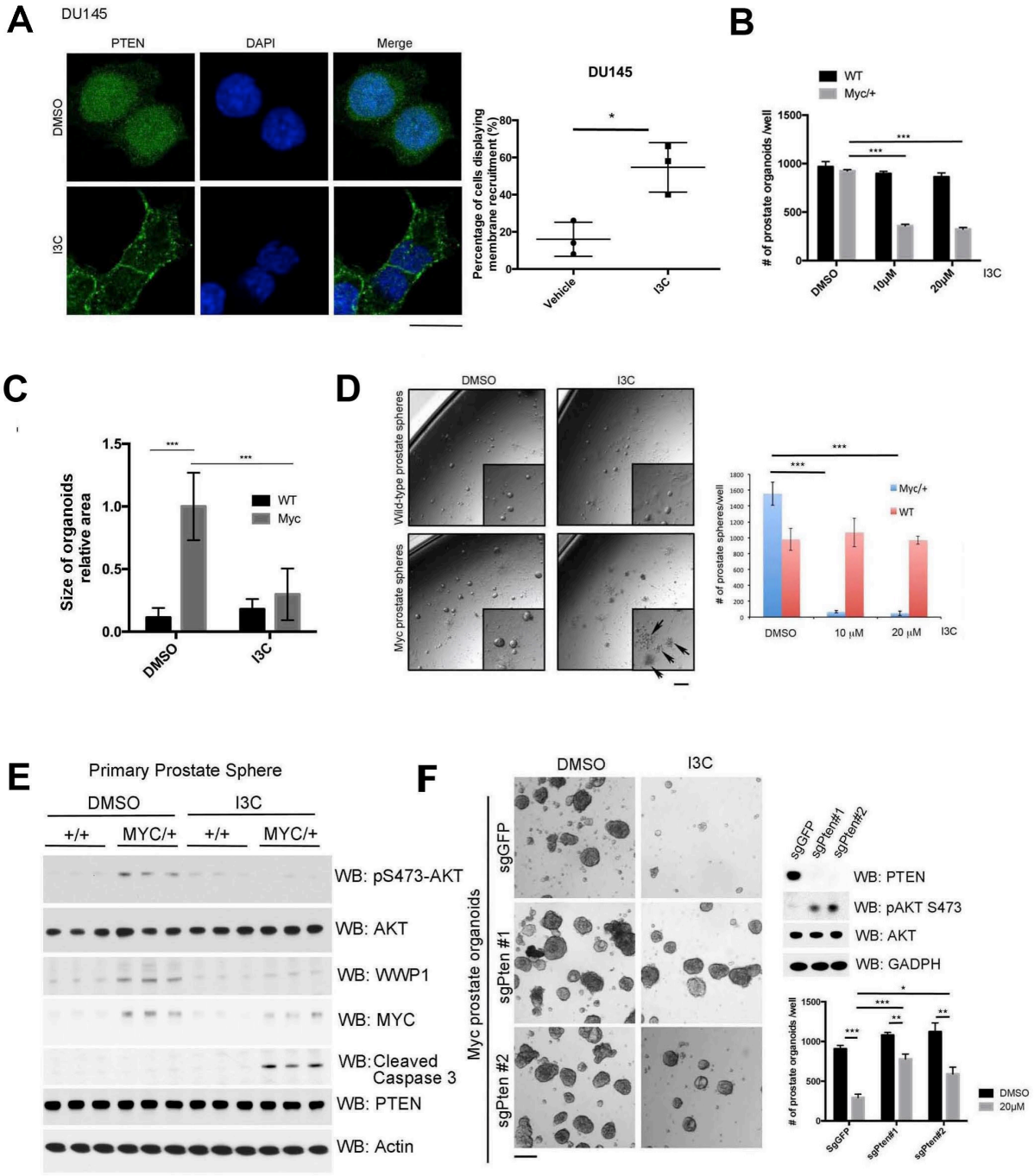
A
DU145
PTEN
DAPI
Merge
DMSO
I3C
DU145
Percentage of cells displaying membrane recruitment (%)
Vehicle
I3C
B
WT
Myc/+
# of prostate organoids /well
DMSO
10μM
20μM
I3C
C
Size of organoids relative area
WT
Myc
DMSO
I3C
D
DMSO
I3C
Wild-type prostate spheres
Myc prostate spheres
# of prostate spheres/well
Myc/+
WT
DMSO
10 μM
20 μM
I3C
E
Primary Prostate Sphere
DMSO
I3C
+/+
MYC/+
+/+
MYC/+
WB: pS473-AKT
WB: AKT
WB: WWP1
WB: MYC
WB: Cleaved Caspase 3
WB: PTEN
WB: Actin
F
DMSO
I3C
Myc prostate organoids
sgGFP
sgPten #1
sgPten #2
sgGFP
sgPten#1
sgPten#2
WB: PTEN
WB: pAKT S473
WB: AKT
WB: GADPH
# of prostate organoids /well
DMSO
20μM

Fig. S8.

(**A**) I3C on PTEN subcellular localization in DU145 cells. DU145 cells treated with 20 μM I3C every other day for 4 Days. Confocal images of DU145 cells treated with/without I3C were stained with DAPI and the indicated antibodies (left panel). Bar, 20 μm. The percentage of cells displaying PTEN plasma membrane localization was quantified (right panel). Data are mean ± SD; triplicate experiments, fifty cells per group per experiment (**P<0.005, *P<0.05, n=50, Student's t-tests).

(**B**) Analysis the effects of I3C on prostate organoids forming ability from WT or Hi-Myc mice treated with/without 10 μM or 20 μM I3C every other day for 3 Days. The organoids numbers were quantified and presented as mean ± SD (***P<0.0005, **P<0.005, n=50 organoids, Student's t-tests).

(**C**) Analysis the effects of I3C on prostate organoids size from WT or Hi-Myc mice treated with/without 20 μM I3C for 3 Days. The organoids numbers were quantified and presented as mean ± SD (***P<0.0005, **P<0.005, n=50 organoids, Student's t-tests).

(**D**) Analysis of I3C on prostate sphere forming ability of WT or Hi-Myc prostate prostatic epithelial cells. The boxed areas are enlarged two folds to show the morphologies of the prostate spheres at P1 passage treated with/without 10 μM I3C every other day for 3 Days. Arrow indicates the apoptotic cells (left). Bar, 20 μm. The sphere numbers were quantified and presented as ± SD (***P<0.0005, **P<0.005. triplicate experiments, Student's t-tests) (right).

(**E**) Western blot analysis of prostate spheres at P1 passage treated with 20 μM I3C every other day for 3 Days.

(**F**) Analysis the effects of *Pten* deletion on prostate organoids forming ability from Hi-Myc mice by CRISPR. Bar, 100 μm (left). Western blot analysis with indicated organoids was included on the right. The organoids numbers were quantified and presented as mean ± SD (***P<0.0005, **P<0.005, *P<0.05, triplicate experiments, Student's t-tests) (right bottom).

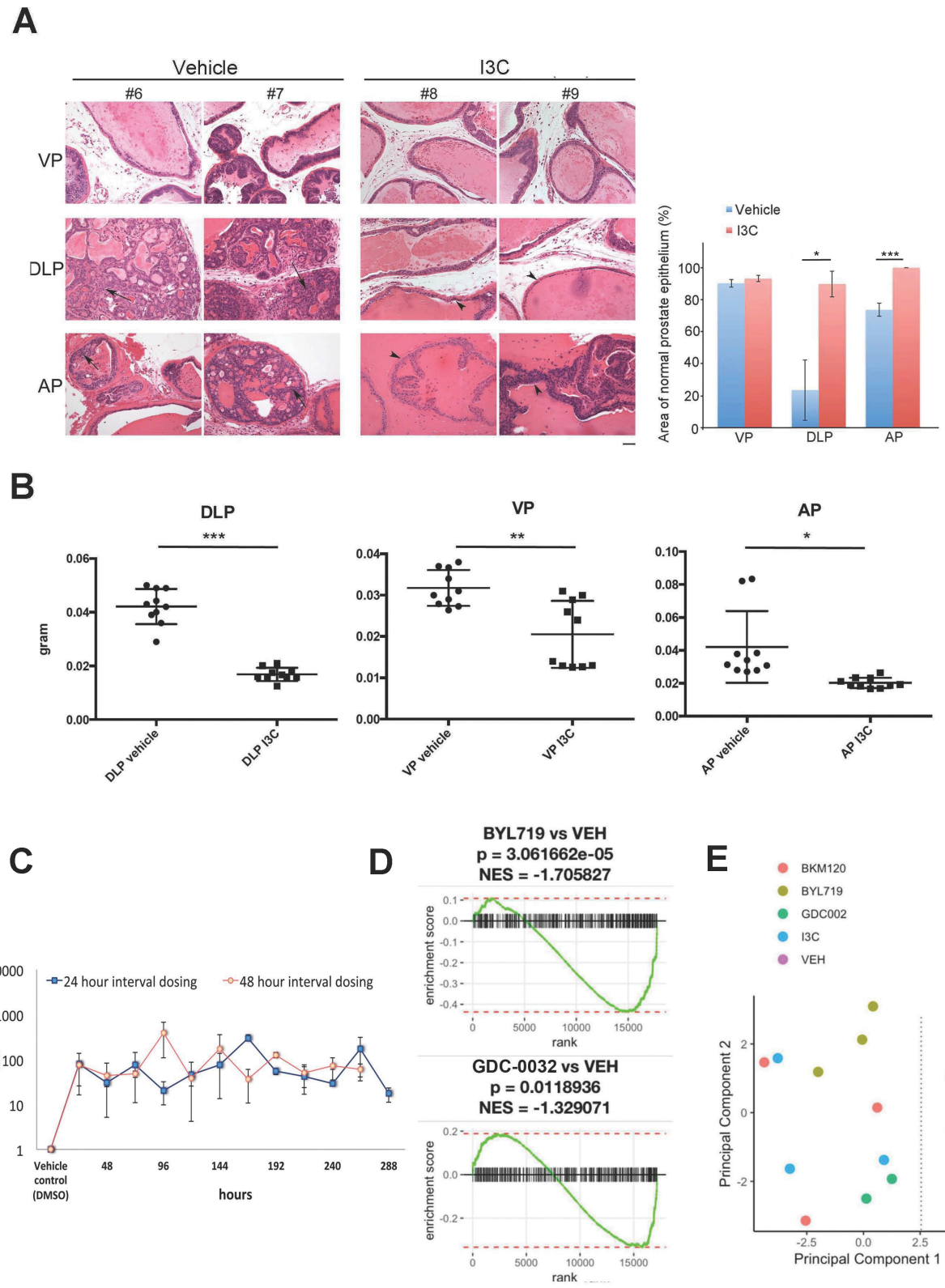
A
Vehicle
I3C
#6
#7
#8
#9
VP
DLP
AP
Vehicle
I3C
Area of normal prostate epithelium (%)
VP
DLP
AP
B
DLP
VP
AP
gram
DLP vehicle
DLP I3C
VP vehicle
VP I3C
AP vehicle
AP I3C
C
24 hour interval dosing
48 hour interval dosing
nM
Vehicle control (DMSO)
hours
D
BYL719 vs VEH
p = 3.061662e-05
NES = -1.705827
GDC-0032 vs VEH
p = 0.0118936
NES = -1.329071
enrichment score
rank
E
BKM120
BYL719
GDC002
I3C
VEH
Principal Component 2
Principal Component 1

Fig. S9.

(**A**) H&E staining of mouse prostates. Quantification of percentage of normal epithelium in Hi-Myc mice treated with vehicle or I3C at 6 months as shown in Fig. 5D. The mice at 5 months of age were treated I. P. with I3C (20 mg/kg), three times a week for 1 month stariting on Day zero. Representative pictures were shown in the panel. Data are mean ± SD; n=3 per group. (**P<0.005, *P<0.05, Student's t-tests). Scale bar, 50 μm.

(**B**) Analysis of the weight of the prostate lobes derived from Hi-Myc mice treated with vehicle or I3C. The mice at 5 months of age were treated I.P. with I3C (20 mg/kg), three times a week for 1 month starting on day zero. (n=5 per genotype). (***P<0.0005, **P<0.005, *P<0.05, Student's t-tests).

(**C**) Daily plasma concentration (Mean±SD) of I3C following intraperitoneal administration at 20 mg/kg everyday or every other day. (24 hour interval dosing versus 48 hr interval dosing).

(**D**) Gene set enrichment analysis (GSEA) of RNA-Seq data from the DLP prostates of (1) BYL719 treated mice versus vehicle treated and (2) GDC-0032 treated mice versus vehicle treated mice using the PI3K-AKT signaling pathway gene set annotated in the Kyoto Encyclopedia of Genes and Genomes (KEGG). Mice from all groups contain the same Hi-Myc genetic background unless otherwise noted.

(**E**) First two principal components of the expression levels of the PI3K-AKT signaling pathway genes across five groups of mice: I3C-treated mice, BKM120-treated mice, BYL719-treated mice, GDC-0032-treated mice and vehicle-treated mice. Mice from all four groups contain the same Hi-Myc genetic background unless otherwise noted.

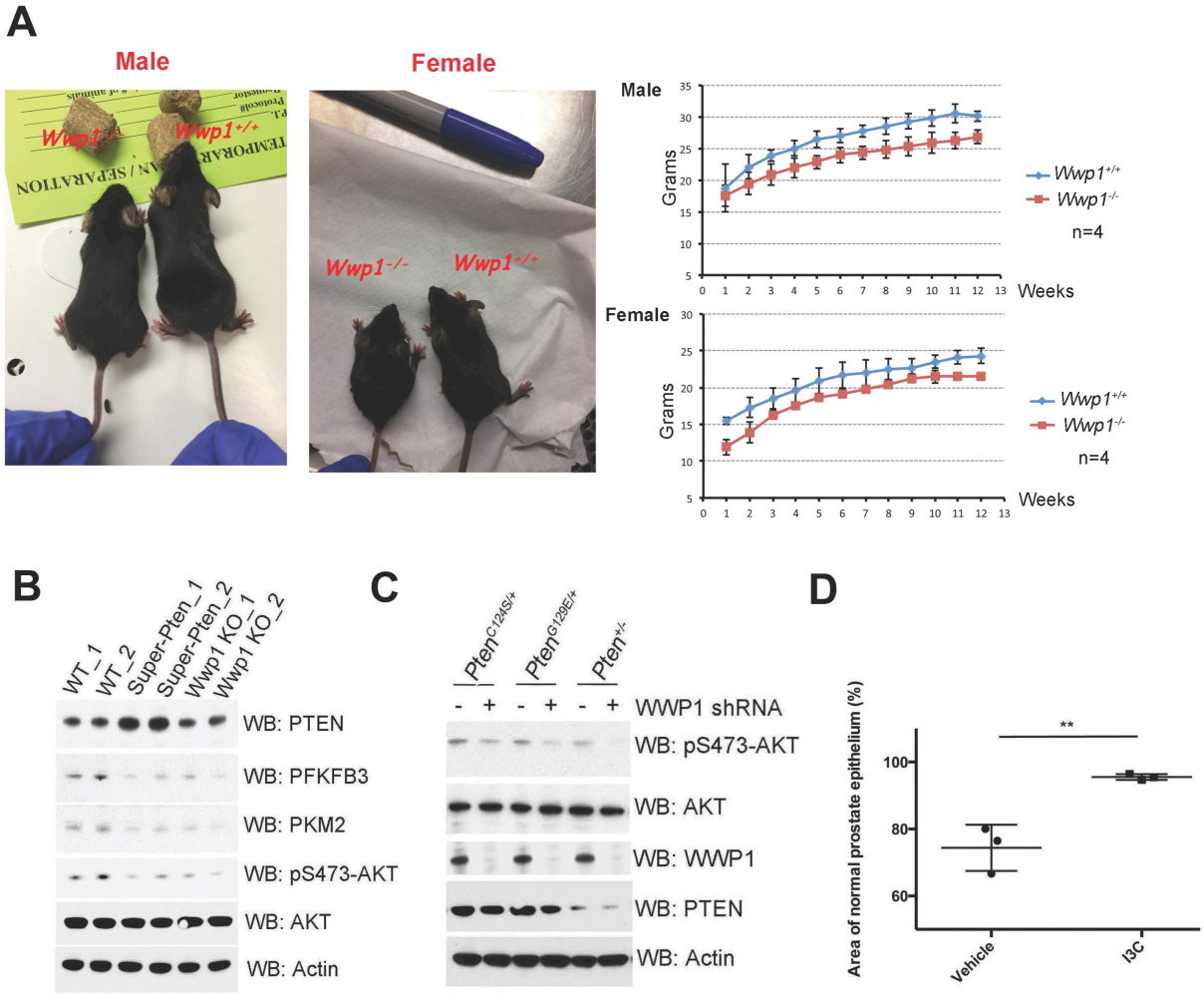
A
Male
Female
Wwp1-/-
Wwp1+/+
Male
Female
Grams
Weeks
n=4
B
WT_1
WT_2
Super-Pten_1
Super-Pten_2
Wwp1 KO_1
Wwp1 KO_2
WB: PTEN
WB: PFKFB3
WB: PKM2
WB: pS473-AKT
WB: AKT
WB: Actin
C
WWP1 shRNA
WB: pS473-AKT
WB: AKT
WB: WWP1
WB: PTEN
WB: Actin
D
Area of normal prostate epithelium (%)
Vehicle
I3C
**

Fig. S10.

(**A**) Growth curves indicate that *Wwp1* KO results in reduced body mass.

(**B**) Western blot analyses of MEFs with different genotypes with indicated antibodies.

(**C**) Western blot analyses of AKT activation in MEFs with different genetic backgrounds upon WWP1 knockdown.

(**D**) Quantification of percentage of normal epithelium in $Pten^{+/-}$ mice treated with vehicle or I3C at 8.5 months as shown in Fig. 5J. The mice at 7.5 months of age were treated I. P. with I3C (20 mg/kg), three times a week for 1 month starting on Day zero. Representative pictures were shown in the panel. (n=3 per group)). (***P<0.0005, **P<0.005, *P<0.05, Student's t-tests). Scale bar, 50 μm.

Supplementary Table S1.

List of PTEN associated proteins identified by Mass spectrometric analysis

TBC1 domain family member 4 (TBC1D4)	Chromosome 13q 22.2
HECT-type ubiquitin E3 ligase WWP1 (WWP1)	Chromosome 8q 21.3
Sperm-associated antigen 5 (SPAG5)	Chromosome 17q 11.2
Synaptotagmin-like protein 4 (SYTL4)	Chromosome Xq 22.1
Telomere-associated protein RIF1 (RIF1)	Chromosome 2q 23.3
Huntingtin-interacting protein 1-related protein (HIP1R)	Chromosome 12q 24.31
Heterogeneous nuclear ribonucleoprotein U-like protein 1 (HNRNPUL1)	Chromosome 19q 13.2
Nedd4 like E3 ubiquitin E3 ligase NEDD4-1 (NEDD4)	Chromosome 15q 21.3
ATP-dependent RNA helicase A (DHX9)	Chromosome 1q 25.3
Poly [ADP-ribose] polymerase 1 (PARP1)	Chromosome 1q 42.12
Isoform 2 of Telomere-associated protein RIF1 (RIF1)	Chromosome 2q 23.2
Structural maintenance of chromosomes protein 3 (SMC3)	Chromosome 10q 25.2
C-1-tetrahydrofolate synthase (MTHFD1)	Chromosome 14q 23.3
Isoform p135 of Dynactin subunit 1 (DCTN1)	Chromosome 2p 13.1
Clustered mitochondria protein homolog (CLUH)	Chromosome 17p 13.3
Isoform 2 of DNA repair protein RAD50 (RAD50)	Chromosome 5q 31.1
Structural maintenance of chromosomes protein 1A (SMC1A)	Chromosome xp 11.22
Isoleucine-tRNA ligase (IARS)	Chromosome 9q 22.31
Isoform 2 of Structural maintenance of chromosomes protein 2 (SMC2)	Chromosome 9q 31.1
Isoform 2 of Putative RNA-binding protein 15 (RBM15)	Chromosome 1p 13.3
Monofunctional C1-tetrahydrofolate synthase (MTHFD1L)	Chromosome 6q 25.1
Cytoskeleton-associated protein 4 (CKAP4)	Chromosome 12q 23.3
Heat shock protein 70 kDa protein 6 (HSPA6)	Chromosome 1q 23.3